

Extending validity of X-ray in-line phase tomography to heterogeneous objects

MAX LANGER^{1,2,*}, BERNHARD HESSE^{1,2,3}, ALEXANDRA PACUREANU⁴, HEIKKI SUHONEN², PETER CLOETENS²,
KAY RAUM³, AND FRANÇOISE PEYRIN^{1,2}

¹Laboratoire 1 Université de Lyon, Creatis ; CNRS UMR 5220 ; INSERM U 1022 ; Université Lyon 1 ; INSA Lyon ; 7 avenue Jean Capelle, F-69621 Villeurbanne, France

²European Synchrotron Radiation Facility, 6 rue Jules Horowitz, F-38043 Grenoble, France

³Julius-Wolff-Institute & Berlin-Brandenburg School for Regenerative Therapies, Charité – Universitätsmedizin Berlin, Augustenburger Platz 1, D-13353 Berlin, Germany

⁴Centre for Image Analysis & SciLife Laboratory, Uppsala University, Box 337, SE-75105, Sweden

¹max.langer@esrf.fr, bernhard.hesse@esrf.fr, peyrin@esrf.fr

²cloetens@esrf.fr, suhonen@esrf.fr

³kay.raum@charite.de

⁴alexandra.pacureanu@cb.uu.se

We present a new way to introduce prior information in the object domain that extends applicability of phase retrieval to some classes of heterogeneous objects. A prior specifically for bone and soft tissue imaging is defined, where the relationship between attenuation and refractive indices is found to follow a power law. We obtain better reconstructions, both qualitatively and quantitatively, on a test object imaged with synchrotron radiation hard X-rays at the European Synchrotron Radiation Facility (ESRF), Grenoble, France. Further, the proposed method is applied to the imaging of bone and soft tissue in samples from a bone healing study, where reconstruction quality is strongly improved.

1 Introduction

In X-ray in-line phase tomography, the aim is to reconstruct the phase of a coherent X-ray beam, which can then be used to tomographically reconstruct the real part of the refractive index distribution in an object [1]. The main interest in this technique is the possible several orders of magnitude increase in sensitivity compared to standard, attenuation based tomography. In the in-line technique, phase contrast is generated by letting the beam propagate in free space a relatively short distance after interaction with the object (Fig. 1) [2]. The measured intensity can be modelled in the Fresnel diffraction formalism, hence the images recorded can be called Fresnel diffraction patterns. Several algorithms for phase retrieval from Fresnel diffraction patterns have been developed. Most of these rely on linearization of the Fresnel integral to yield efficient algorithms [1, 3-7].

Due to the weak transfer of low spatial frequencies in the phase by the Fresnel transform, phase retrieval from Fresnel diffraction patterns is inherently sensitive to noise in the low frequency range. A typical situation is shown in Fig. 3a. This has previously been addressed by introducing a scaled version of the attenuation image as prior knowledge on the phase, essentially assuming a homogeneous object. Recently, we proposed to instead introduce the prior knowledge in the object domain, thus allowing for heterogeneous samples, that is the ratio between attenuation and refractive indices is allowed to vary across the sample. Previously, a prior based on segmentation of the attenuation scan to achieve an estimate of the object composition was

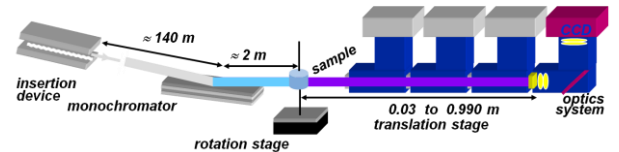


Figure 1 : Experimental setup. Synchrotron radiation X-rays are monochromated and used to image a sample mounted on a rotation stage for tomographic imaging. The detector is mounted on a translation stage to allow for in-line phase contrast.

presented [8]. This essentially allows for multi-material objects.

Here, we extend this approach to heterogeneous objects. Instead of thresholding the attenuation scan, knowledge of the object composition is used to find an empirical relationship between the attenuation index β and refractive index δ . The a priori phase maps are constructed by first reconstructing the attenuation index, applying the found empirical relationship to yield an initial guess of the refractive index, and finally forward project this estimate at each projection angle. The phase is then retrieved using a phase retrieval algorithm such as the mixed approach [5], using the a priori phase maps in the regularization term.

2 Materials and Methods

Considering a monochromatic, coherent, parallel X-ray beam, the optical properties of an object can be described by its complex refractive index

$$n(\mathbf{r}) = 1 - \delta_n(\mathbf{r}) - i\beta(\mathbf{r}) \quad (1)$$

where $\mathbf{r} = (r, s, t)$ are the spatial coordinates in the object domain. The X-ray interaction with the object can at each projection angle θ be described by a transmittance function

$$T_\theta(\mathbf{x}) = a_\theta(\mathbf{x}) \exp[i\varphi_\theta(\mathbf{x})] = \exp[-B_\theta(\mathbf{x}) + i\varphi_\theta(\mathbf{x})] \quad (2)$$

where the attenuation $a_\theta(\mathbf{x})$ and phase shift $\varphi_\theta(\mathbf{x})$ are projections through the real and imaginary parts of $n(\mathbf{r})$:

$$\begin{aligned} B_\theta(\mathbf{x}) &= (2\pi/\lambda) \int_{(\theta,\mathbf{x}) \text{ line}} \beta_n(\mathbf{r}) dz \text{ and} \\ \varphi_\theta(\mathbf{x}) &= -(2\pi/\lambda) \int_{(\theta,\mathbf{x}) \text{ line}} \delta_n(\mathbf{r}) dz \end{aligned} \quad (3)$$

where $z = r \cos \theta + s \sin \theta$ is the propagation direction of the X-rays. Free space propagation over distance D after interaction with the object can be described by the Fresnel transform

$$T_{\theta,D}(\mathbf{x}) = \text{Fr}_D[T(\mathbf{x})] \quad (4)$$

What can be measured, however, is the intensity $I_D(\mathbf{x})$ of the wavefield:

$$I_D(\mathbf{x}) = |T_{\theta,D}(\mathbf{x})|^2 + \gamma(\mathbf{x}), \quad (5)$$

where $\gamma(\mathbf{x})$ accounts for noise and other imperfections in the image (these contributions, however, are not necessarily additive or independent of the object). Setting $D = 0$ yields directly the attenuation image

$$I_0(\mathbf{x}) = a_\theta^2(\mathbf{x}) + \gamma(\mathbf{x}) \quad (6)$$

familiar from standard tomography. The phase shift can be reconstructed from a series of images at different distances by solving the minimization problem

$$\hat{\varphi}_\theta(\mathbf{x}) = \arg \min \sum_D |\tilde{I}_{\theta,D,\varphi}(\mathbf{x}) - I_{\theta,D}(\mathbf{x})|^2 + \alpha |\varphi_\theta(\mathbf{x}) - \varphi_{\theta,0}(\mathbf{x})|^2 \quad (7)$$

where $\tilde{I}_{\theta,D,\varphi}(\mathbf{x})$ is the intensity calculated e.g. the mixed approach [5] and $\varphi_{\theta,0}(\mathbf{x})$ is an a priori known solution.

To allow for a heterogeneous object, the a priori knowledge has to be introduced in the object domain [8]. Here, we set the δ/β -ratio directly as a function of β , hence letting it vary across the sample. The a priori phase maps are generated based on a reconstructed attenuation scan. Reconstructing $\beta(\mathbf{r})$ from $I_{\theta,0}(\mathbf{x})$ yields

$$\hat{\beta}(\mathbf{r}) = \beta(\mathbf{r}) + \Gamma(\mathbf{r}), \quad (8)$$

where $\Gamma(\mathbf{r})$ is noise and other imperfections due to $\gamma(\mathbf{x})$. The relationship between attenuation and refractive indices is introduced as a function $m(\mathbf{r})$, so that the a priori estimate of $\delta(\mathbf{r})$ is obtained as

$$\delta_0(\mathbf{r}) = m(\mathbf{r})\hat{\beta}(\mathbf{r}). \quad (9)$$

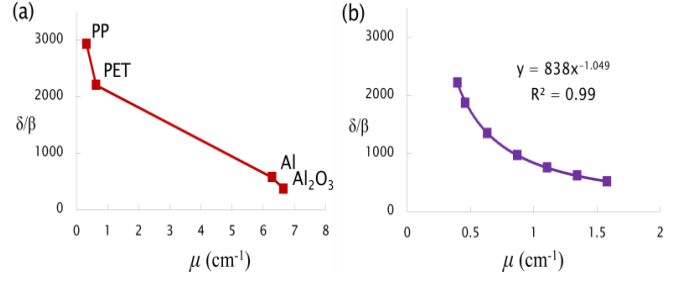


Figure 2 : Empirical relationships from attenuation to δ/β at the respective energies. (a) For the test object, a simple relationship cannot be found. Here, we use linear interpolation between the known materials to achieve a mapping. (b) In bone, the δ/β is found to follow a power law.

In this work, we consider two types of objects : a test object constructed from fibers of Al, Al₂O₃, PET and PP, and bone samples with soft tissue (specifically for the study of healing). In the test object, no empirical relation can be found. Here, we let $m(\mathbf{r})$ vary as the linear interpolation between the theoretical values (Fig. 2a). In bone, on the other hand, we can find an empirical relationship for $m(\mathbf{r})$. We assume a simplified composition of bone, consisting of a fixed weight fraction of collagen and a variable balance of water and hydroxylapatite (the mineral constituent of bone), ranging from only water in soft tissue to only mineral in fully mineralized bone. Under this assumption, we find that the relationship between attenuation and refractive index follows a power law (fig. 2b). For phase retrieval, the prior estimates of the phase at each projection angle is obtained by forward projection as

$$\varphi_{\theta,0}(\mathbf{x}) = -(2\pi/\lambda) \int_{(\theta,\mathbf{x}) \text{ line}} \delta_0(\mathbf{r}) dz. \quad (10)$$

The two samples were imaged at the ID19 beamline of the European Synchrotron Radiation facility (ESRF), Grenoble, France. In both cases, a double Si crystal monochromator was used to achieve a high degree of monochromaticity. A detector consisting of a scintillating screen for X-ray to visible light conversion, conventional visible light microscope optics and a 2048×2048 pixels CCD, was used for imaging. The test object was imaged at 0.7 μm pixel size with an X-ray energy of 22.5 keV, using four propagation distances ($D=[2 \ 10 \ 20 \ 45]$ mm), and 1500 projections over a 180 degree rotation. The bone sample was imaged at 5 μm pixel size with an X-ray energy of 27 keV, three propagation distances ($D=[60, \ 300, \ 999]$ mm), and 2000 projections over a 360 degree rotation.

3 Results

The test object was reconstructed using the mixed approach [5], the mixed approach with the homogeneous object prior [9], Paganin's method for homogeneous objects [4], and the proposed method. The δ/β -ratio was set to 367, corresponding to Al for the homogeneous object approaches. Reconstructed slices are shown in Fig. 3. The mixed approach reconstruction (Fig. 3a) shows a very sharp

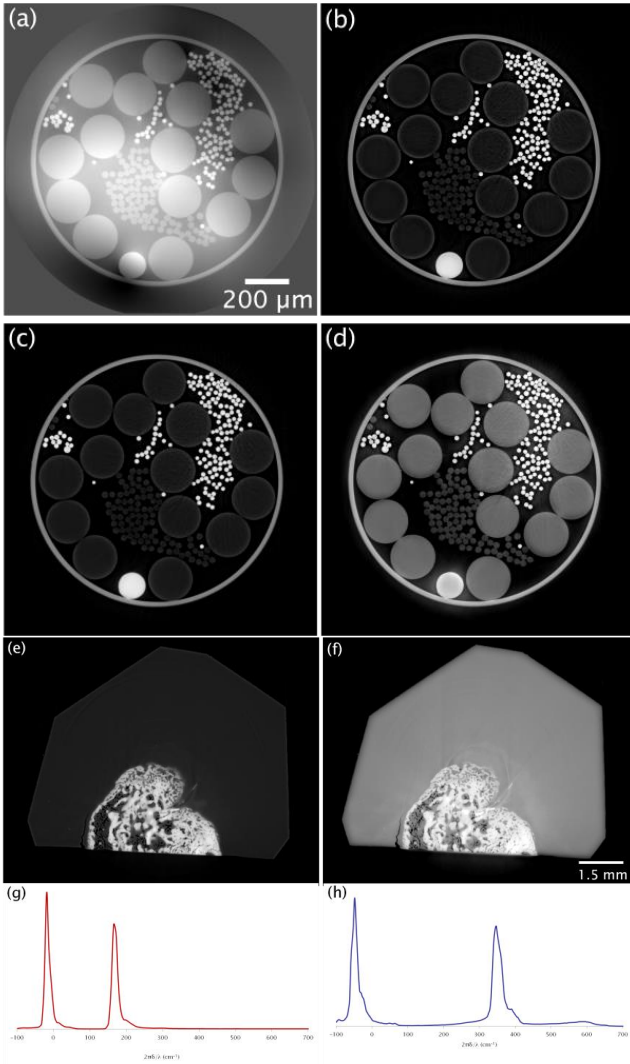


Figure 3 : Reconstructed slices of the test object. (a) Using the mixed approach (b) mixed approach with homogeneity prior, (c) Paganin's method and (d) the proposed method. Reconstructed slices and corresponding histograms of the bone sample with (e, g) Paganin's method and (f, h) the proposed method.

reconstruction, but is contaminated with characteristic low frequency noise. The homogeneous object approaches (Fig 3b, c) clearly improves the low frequency behaviour, but under-estimates values in, and leaves fringes around, zones where the δ/β -ratio is selected too low (i.e. the plastics). With the proposed method, this deficiency is alleviated and strong area contrast is visible between the different materials. Quantitative evaluation of image quality is presented in Table 1. Note that the reconstruction with the proposed method does not achieve as good accuracy as the attenuation, but several times better than the homogeneous approaches. The proposed method reaches an order of magnitude improvement in precision, however.

Tab 1 : Reconstruction quality for the different algorithms

	Local normalized error and relative standard deviation (%)				Total
	Al	Al ₂ O ₃	PET	PP	
Attenuation	1.50 (14.5)	-4.42 (17.5)	14.6 (130)	9.09 (274)	7.40 (92.5)
Mixed/homogeneous Al	-2.90 (4.86)	-28.7 (7.37)	-75.8 (27.6)	-64.6 (24.6)	43.0 (14.0)
Paganin Al	-3.31 (5.44)	-0.320 (5.26)	22.5 (21.8)	129 (7.33)	38.7 (11.1)
Mixed/proposed prior	8.02 (5.00)	-13.4 (7.97)	2.33 (9.55)	-24.5 (19.3)	12.0 (9.25)

Reconstructed slices of the bone sample and corresponding histograms using Paganin's method with $\delta/\beta = 516$, corresponding to fully mineralized bone (e, g), and the proposed method (f, h) is shown in fig. 3. Also here, the homogeneous object approach yields fringes on the edges of materials where the selected δ/β -ratio is too low, as in the embedding material. The proposed method, on the other hand, correctly reconstructs both soft and hard tissue. This can be seen from the histogram, as the peak corresponding to the embedding material is correctly placed, and a peak corresponding to bone is visible.

4 Conclusion

We presented a new prior term for in-line phase tomography. We showed that for certain classes of samples, such as bone, empirical relationships can be found between the attenuation and refractive indices. We evaluated the method on a test object and in the imaging of bone samples for bone healing studies, and found that the proposed method improved reconstructions both qualitatively and quantitatively. Future work includes combination with non-linear iterative optimization to further reduce the object assumptions, improve reconstruction accuracy, and achievable spatial resolution.

5 References

1. P. Cloetens, W. Ludwig, J. Baruchel, D. Van Dyck, J. Van Landuyt, et al., Appl. Phys. Lett. **75**, 2912 (1999).
2. A. Snigirev, I. Snigireva, V. Kohn, S. Kuznetsov, and I. Schelokov, Rev. Sci. Instrum. **66**, 5486 (1995).
3. K. A. Nugent, T. E. Gureyev, D. F. Cookson, D. Paganin, and Z. Barnea, Phys. Rev. Lett. **77**, 2961 (1996).
4. D. Paganin, S. C. Mayo, T. E. Gureyev, P. R. Miller, and S. W. Wilkins, J. Microsc. **206**, 33 (2002).
5. J. P. Guigay, M. Langer, R. Boistel, and P. Cloetens, Opt. Lett. **32**, 1617 (2007).
6. M. Langer, P. Cloetens, J. P. Guigay, and F. Peyrin, Med. Phys. **35**, 4556 (2008).
7. X. Wu, H. Liu, A. Yan, Opt. Lett. **30**, 379 (2005).
8. M. Langer, P. Cloetens, A. Pacureanu, and F. Peyrin, Opt. Lett. **37**, 2151 (2012).
9. M. Langer, P. Cloetens, and F. Peyrin, IEEE Trans. Image Process. **19**, 2428 (2010).